의학석사 학위논문

Predicting Human Epidermal Growth Factor Receptor Status with Functional Imaging Modalities; ^{68}Ga-RGD PET/CT, Dynamic Contrast-Enhanced and Diffusion-Weighted MRI

유방암에서 ^{68}Ga-RGD PET/CT, 동적조영증강 및 확산강조 MRI를 이용한 외피성장인자수용체 발현 예측

2012년 8월

서울대학교 대학원

의학과 핵의학 전공

윤 혜 전

유방암에서 ^{68}Ga-RGD PET/CT, 동적조영증강 및 확산강조 MRI를 이용한 외피성장인자수용체 발현 예측

Predicting Human Epidermal Growth Factor Receptor Status with Functional Imaging Modalities; ^{68}Ga-RGD PET/CT, Dynamic Contrast-Enhanced and Diffusion-Weighted MRI

지도교수 강 건 욱

이 논문을 의학석사 학위 논문으로 제출함

2012년 4월

서울대학교 대학원

의학과 핵의학 전공

윤 혜 전

윤혜전의 의학 석사 학위논문을 인준함

2012년 6월

위원장 _____ (인)

부위원장 _____ (인)

위원 _____ (인)

Predicting Human Epidermal Growth Factor Receptor Status with Functional Imaging Modalities; ^{68}Ga-RGD PET/CT, Dynamic Contrast-Enhanced and Diffusion-Weighted MRI

By Hai Jeon Yoon, M.D.

(Directed by Professor Keon Wook Kang, M.D.)

A Thesis submitted in Partial Fulfillment of the Requirement for the Degree of Master of Philosophy in Medicine (Nuclear Medicine) to Seoul National University College of Medicine

June 2012

Approved by Thesis Committee:

Professor _____Chairman

Professor _____Vice chairman

Professor _____

ABSTRACT

Predicting Human Epidermal Growth Factor Receptor Status with Functional Imaging Modalities; ^{68}Ga-RGD PET/CT, Dynamic Contrast-Enhanced and Diffusion-Weighted MRI

Yoon, Hai-jeon

College of Medicine, Department of Nuclear Medicine

The Graduate School

Seoul National University

Purpose: The subset of patients with HER2 over-expression is expected to show rapid tumor growth, frequent lymph node metastasis and can be candidates for trastuzumab treatment. HER1/EGFR is known to share extensive sequence homology with HER2. This prospective study purposed to investigate the correlation of quantitative parameters derived from functional

imaging modalities reflecting tumor angiogenesis, which is an important mechanism of tumor progression, with HER expression identified from histopathology. And the association of imaging parameters with vascular endothelial growth factor (VEGF) expression, a representative angiogenic biomarker, was also investigated.

Methods: Thirty-seven locally advanced breast cancer patients (47.8 ± 7.6 year-old) who were scheduled with neoadjuvant chemotherapy were prospectively enrolled in this study. ^{68}Ga-RGD PET/CT, dynamic contrast-enhanced (DCE) and diffusion-weighted (DW) MRI were performed before treatment. Tumor to background ratio (TBR) from RGD PET, transfer constant [K_{trans}], extravascular extracellular fractional volume [V_e], rate constant [K_{ep}] and initial area under curve ($_{i}$AUC) from DCE MRI, apparent diffusion coefficient (ADC_{Mean}) value from DW MRI were used as quantitative imaging parameters. Clinical factors including tumor size, lymph node status, estrogen receptor status were also considered. Core needle biopsy was performed for pathologic confirmation. HER expression was identified with immunohistochemistry (IHC). For more accurate HER2 status evaluation, equivocal IHC cases were referred to additional fluorescence in situ hybridization (FISH) analysis. The association of each clinical and imaging

parameter with HER expression was assessed. Linear regression and reciever operating characteristics (ROC) analyses were used to evaluate each parameter's predictive strength and predictive performance for HER expression. Furthermore, IHC staining for VEGF was performed to evaluate the association between imaging parameters and VEGF expression.

Results: Among 37 patients, HER2 over-expression was identified in 13 patients. And HER1/EGFR expression was identified in 8 of 31 patients. TBR was significantly higher in HER positive group than negative group (p<0.001 for HER1/EGFR and p=0.002 HER2). However, none of MR parameters showed significant differences. Predictive performace of TBR regarding HER2 expression was 92.3% sensitivity, 70.8% specificity (AUC 0.849). Regarding HER1/EGFR, 87.5% sensitivity, 69.6% specificity was resulted (AUC 0.870). HER2/CEP17 ratio counted from FISH analysis was available in 28 patients (2.7±2.8, range 0.7-9.3). Moderate positive correlation existed between TBR and HER2/CEP17 ratio (r=0.64, p=0.0002), while moderate negative correlation existed between ADC_{Mean} and HER2/CEP17 ratio (r=-0.65, p=0.0004). In total group, predictive strength (R^2) of TBR and ADC_{Mean} against HER2 ratio was 0.41 and 0.43, respectively. In HER2 positive subgroup, R^2 value was 0.708 for TBR and 0.794 for ADC_{Mean}. IHC staining for

VEGF was performed in 20 specimens. Strong VEGF expression was significantly associated with high TBR in RGD PET/CT (p=0.016), while none of MR parameters showed significant associations. No direct association was noted between HER2 and VEGF expression. However, HER1/EGFR expression showed significant correlation with VEGF expression (p=0.06).

Conclusion: ^{68}Ga-RGD PET/CT and DW MRI can be used for HER biomarker prediction. Especially, ^{68}Ga-RGD PET/CT showed high predictive value for HER1/EGFR as well as HER2 by reflecting angiogenic activity. Although the predictive strength was insufficient for immediate diagnostic application, these results warrant further investigation on the potential of functional imaging modalities to facilitate noninvasive assessment of molecular target expression in breast cancer. Furthermore, this study suggests the potential role of HER in angiogenic pathway.

Key Words: RGD PET, Dynamic Contrast-Enhanced MRI, Diffusion-Weighted MRI, Biomarker, Angiogenesis

Student Number: 2010-21810

LIST OF TABLES

LIST OF FIGURES

LIST OF ABBREVIATIONS

HER: Human epidermal growth factor receptors

VEGF: Vascular endothelial growth factor

PET: Positron emission tomography

MRI: Magnetic resonance imaging

RGD: Arginine-glycine-aspartic acid

DCE: Dynamic contrast-enhanced

DW: Diffusion-weighted (DW)

K_{trans}: Contrast agent transfer rate between blood and tissue

V_e: Extravascular extracellular fractional volume

K_{ep}: Contrast agent backflux rate constant

$_{i}$AUC: Initial area under curve

ROI: Region of interest

EPI: Echo planar imaging sequence

VOI: Volume of interest

ADC: Apparent Diffusion Coefficient

IHC: Immunohistochemistry

FISH: Fluorescence in situ hybridization

CONTENTS

I. INTRODUCTION

Breast cancer has complex and heterogeneous phenotypes manifesting a wide range of variation in patient's prognosis and outcome. Therefore, personalized therapy according to specific phenotype is crucial to improve disease control in breast cancer. To select the candidates most likely to benefit from personalized targeted therapy, specific biomarker identification is required. Furthermore, specific biomarker status can also provide information regarding treatment response and prognosis, thereby assisting patient stratification.

Human epidermal growth factor receptors (HER) are important tissue biomarkers in breast cancer. Of HER family, the most famous receptor is HER2 (also known as c-erbB-2), which over-expressed in 25-30% of breast cancers. HER2 over-expression is closely related with tumor progression, poor prognosis and resistance to hormonal or chemotherapy (1). HER2 over-expressed patients are candidates of trastuzumab, a humanized monoclonal antibody targeting HER2 receptor protein. HER1 (also known as epidermal growth factor receptor, EGFR) is another member of ErbB receptor family and share extensive sequence homology with HER2 (2). The formation

of heterodimers among HER subtypes initiates distinct signaling pathways responsible for tumor progression and especially combination of HER1/EGFR and HER2 is the most potent inducer of vascular endothelial growth factor (VEGF) expression and tumor vascularity (3, 4).

Angiogenesis is an important mechanism of tumor progression and VEGF is a representative angiogenic biomarker. There have been suggested preclinical and clinical evidence that "HER2 over-expression" in human malignancy is closely associated with increased angiogenesis by regulating VEGF expression (4, 5).

So far, identification of biomarker expression was performed with a single tumor biopsy. Although it is a current standard method, biopsy has limitations. Repeated examination is limited because of invasiveness, thus it is difficult to evaluate dynamic nature of tumor during treatment. To evaluate the regional heterogeneity of tumor is also limited, because biopsy can reflect only a small part of entire tumor mass.

Therefore, imaging biomarkers derived from functional imaging modalities such as positron emission tomography (PET) and magnetic resonance imaging (MRI) are emerging as potential surrogate markers by providing general, noninvasive, reproducible and quantitative assessment

regardless of tumor location or type. Furthermore, imaging biomarkers can potentialize early prediction of disease prognosis as well as treatment response (6-9). However, exploitation of this technique is still in early stages of development and molecular heterogeneity of breast cancer make difficult verifying appropriate surrogate imaging biomarker for "one-stop staging".

Currently, arginine-glycine-aspartic acid (RGD) PET, dynamic contrast-enhanced (DCE) and diffusion-weighted (DW) MRI are expected as promising functional imaging modalities, especially for angiogenesis evaluation (10-12). Radiolabelled RGD allows non-invasive and highly selective determination of $\alpha_v\beta_3$ integrin, a receptor protein involved in the migration of endothelial cells during angiogenesis (10, 13). A number of quantitative parameters derived from DCE MRI can provide information regarding change of vascular permeability and blood flow during angiogenesis (14, 15). DW MRI enables non-invasive characterization of tumor microenvironment based on water diffusion as a "surrogate marker of cellularity" and was hypothesized that diffusion may have an indirect correlation with VEGF expression and vascular permeability (16, 17).

In this study, I purposed to elucidate quantitative imaging parameters which can predict pathologic tissue biomarkers, especially HER expression, by

applying functional molecular imaging modalities for angiogenesis, ^{68}Ga-RGD PET/CT, DCE and DW MRI. Furthermore, we also investigated the association of those imaging parameters with representative angiogenic biomarker VEGF.

II. MATERIALS AND METHODS

1. Patients

Between August 2010 and March 2012, 41 locally advanced breast cancer patients (cT2-4, Nx, M0) who were scheduled for neoadjuvant chemotherapy and subsequent surgery were prospectively enrolled. Pre-treatment RGD PET and/or DCE and/or DW MRI were performed in addition to current staging modalities including mammography, breast ultrasound and chest CT. All of patients were pathologically confirmed with core needle biopsy. Thirty-seven of them were invasive ductal carcinoma (IDC) and the rest 4 patients were invasive lobular carcinoma (ILC). Four ILC patients were excluded, thereby including 37 IDC patients for further statistical analysis (all female, 47.8 ± 7.6 yrs, range 34-62 yrs). Clinical stage, tumor size, lymph node status and hormonal receptor status were recorded and evaluated as clinical parameters. This is a substudy of "PET-MR fusion imaging and surrogate marker for prediction and monitoring of response to neoadjuvant chemotherapy in breast cancer patients" approved by the Institutional Review Board of the Seoul National University Hospital. Informed consent was

obtained from all of enrolled patients.

After staging work up, patients were treated with docetaxel (60−75 mg/m^2) plus doxorubicin (50−60 mg/m^2) regimen weekly for 6 weeks. At the end of chemotherapy, RGD PET and/or DCE and/or DW MRI were obtained for tumor response evaluation. After 3−4 weeks rest, patients proceeded to surgery.

2. ^{68}Ga-RGD PET/CT and Image Analysis

All patients were injected with ^{68}Ga-NOTA-RGD (148-185 MBq) synthesized using a NOTA-RGD kit, which was manufactured by our institution(18) and PET/CT images were acquired 1 h after the intravenous injection. A CT scan was obtained first and an emission scan was consecutively obtained from skull base to proximal thigh, using dedicated PET/CT scanners (Biograph 40, Siemens). Iterative algorithm was used for PET image reconstruction.

Two experienced nuclear medicine physicians reviewed and analyzed PET/CT images using a workstation equipped with dedicated analysis software (Syngo.via, Siemens). In the PET images, maximal standardized uptake value (SUV_{max}) were measured by placing standardized spheric volumes of interest (VOIs) over the tumor mass (SUV_{tumor}) and the contralateral normal breast parenchyma (SUV_{normal}). Tumor-to-background ratio (TBR) was acquired by dividing SUV_{tumor} with SUV_{normal} and used for further statistical analysis. In the case of unclear tumor margin on RGD PET due to the high background activity or relatively low tumor uptake, a VOI was carefully drawn with reference to the combined CT image.

3. DCE MRI and Image Analysis

All MR examinations were performed using 1.5-T scanner (Signa, GE Medical Systems) and dedicated breast coil. For the dynamic study, gadolinium-DTPA (Magnevist [0.1 mmol per kilogram of body weight], Berlex, Wayne, NJ) contrast agent was administered by a rapid automatic injector through an indwelling IV catheter at a rate of 3 cc/sec. A sagittally oriented 3D spoiled gradient-recalled (3D SPGR) T1-weighted MR images were acquired. The acquisition parameters were: TE/TR = 1.78/3.71 msec, flip angle 20 degrees, field of view 200×200 mm, matrix 256×256, 2 mm section thickness with no gap. Imaging acquisition time per one phase was 11 seconds and total acquisition time of 462 seconds was taken for 42 phases.

DCE-MRI images were reviewed by experienced radiologists of our institution's radiology department. Using workstation equipped with Kinetic Modeling Cine Tool Version 2.0 (GE Medical Systems), the contrast agent transfer rate between blood and tissue (K_{trans}), the extravascular extracellular fractional volume (V_e), the contrast agent backflux rate constant (K_{ep}) were calculated by placing a region of interest (ROI) on the hottest area in each tumor mass. Initial area under curve ($_{i}$AUC) was calculated from the time-signal intensity curve.

4. DW MRI and Image Analysis

DW imaging was obtained with single-shot, echo planar imaging sequence (EPI) with diffusion-sensitizing gradients, with the following parameters: an TR/TE of 10000 / 60.9 msec, an image matrix of 190×190, a field of view of 240×240 mm, a slice thickness of 5 mm with no gap. The number of excitations was 2 and the b values were 0 and 750 sec/mm^2. The acquisition time for DW images covering entire breast was 1 minutes 20 seconds.

All DW images were transferred to the workstation and the DWI sequence was postprcessed with MROncoTreat Version 2.0 software (Siemens Medical Solutions, Erlangen, Germany) for Apparent Diffusion Coefficient (ADC) mapping. The ADC map of each lesion was calculated using previously mentioned two b values. By placing a 3D volume of interest (VOI) regarding tumor volume on an ADC map, mean of each ADC value (ADC_{Mean}) was automatically calculated.

5. Pathologic Assessment of HER Status

Core needle biopsy regarding primary breast tumor was performed for pathologic confirmation in all patients. To identify HER1/EGFR expression, immunohistochemical (IHC) staining was done. HER2 expression was evaluated by using IHC and/or fluorescence in situ hybridization (FISH) protocol.

A re-cut section of paraffin-embedded tissue was stained with H&E, and was bound to commercially available antibodies to HER1/EGFR (Dako, Glostrup, Denmark), c-erbB-2 (Novocastra, Newcastle, UK).

HER1/EGFR staining was graded in a binary fashion and was positive in case of any membrane staining (19). To assess c-erbB-2 (HER2) expression, semiquantitative scoring method was applied as follows: 0 for no membrane staining, 1+ for weak inhomogeneous membrane staining in some of tumor cells, 2+ for weak to moderate membrane staining in a large number of tumor cells, and 3+ for strong complete homogeneous membrane staining in most of tumor cells (20).

Score 1+ and 2+ were considered as equivocal results therefore required additional FISH analysis to confirm gene amplification. PathVysion

HER2 DNA Probe Kit was used for slide processing and result was analyzed according to the manufacturer's instructions with use of an epi-illumination fluorescence microscope with triple-pass filter band (DAPI/green/orange). The counted number of HER2 gene signals (orange) was divided by the number of CEP 17 signals (green) to correct polysomy 17 in counting the same 20 nuclei. If the HER2/CEP17 ratio is more than 2.0, HER2 gene amplification was observed. If the ratio is less than 2.0, HER2 gene amplification was not observed. If the ratio is borderline (1.8-2.2), recount of an additional 20 nuclei and recalculation of the ratio was done. In conclusion, ICH staining of 3+ or HER2/CEP17 ratio of more than 2.0 was recorded as positive HER2 result, while ICH staining of 0 or FISH of less than 2.0 was recorded as negative HER2 result (21).

6. Pathologic Assessment of Angiogenic Biomarker

As an angiogenic biomarker, VEGF expression was investigated. Because IHC staining for VEGF was not included initial study protocol, additional re-cut section of residual paraffin block was requested at our pathology department. In the case of insufficient biopsy specimen for additional staining, some of post-surgical specimens were used for IHC staining. After H&E staining, slides were bound to commercially available antibodies to VEGF (Dako, Glostrup, Denmark).

Positive staining of VEGF should be detected in the cytoplasm. Semiquantitative scoring graded as negative (0), weak (1-6), and strong (7-12) was used, which is the product of the number of positively stained tumor cells (0 for negative; 1 for 1-25%; 2 for 26-50%; 3 for 51-75%; 4 for 76-100%) and the staining intensity (0 for negative; 1 for weak; 2 for moderate; 3 for strong).

7. Statistical Analysis

All statistical analysis was performed by using MedCalc software (Ver. 11.4.4, MedCalc Software, Mariakerke, Belgium). All quantitative values were expressed as mean ± SD and 95% confidence interval (CI), P values less than 0.05 were regarded significant.

The association between histologic biomarker status (HER1/EGFR, HER2 and VEGF) and imaging parameters as well as clinical factors were evaluated. For continuous parameters, the Mann-Whitney test was used. For un-continuous parameters, Fisher's exact test or Chi-square test was used.

The Pearson correlation analysis was used to determine associations between continuous potential predictive parameters and HER2/CEP17 ratio. The strength of correlation of each predictive parameter with HER2 gene ratio was computed as Pearson correlation coefficient. The predictive strength of each imaging parameter for HER2 ratio was tested using simple linear regression to produce an equation where quantitative imaging parameter predicted HER2 outcome. Then, multiple linear regression was used to examine the hypothesis that the combination of imaging parameters would improve prediction of pathologic HER2 gene ratio. The predictive strength of

each model is presented as an R^2 value. The statistical significance of the model in subgroup (HER2-positive and HER2-negative) as well as overall group was specified.

The predictive performance of each parameter was demonstrated by using receiver operating characteristics curve. The area under curve (AUC) was calculated and the optimal cut-off value was determined as the point on the curve yielding the best sensitivity and specificity.

III. RESULTS

1. Clinical Features and Outcomes

Thirty-seven IDC patients were included in the analysis. The clinical characteristics of the 37 patients including clinical stage, tumor size, lymph node status and hormonal receptor status are summarized in Table 1.

According to IHC and/or FISH results, HER2 over-expression was detected in 13 of 37 patients (HER2 positive subgroup), while HER2 over-expression was absent in the rest 24 patients (HER2 negative subgroup). All of IHC 1+ (n=10), 2+ (n=12) and some of 3+ (n=6) cases were proceeded to additional FISH analysis. Therefore, HER2/CEP17 ratio was available in 28 patients. HER1/EGFR was positive in 8 of 31 patients. Additional VEGF identification was available in 15 patients. All of 20 patients presented weak to strong VEGF expression (7 weak, 13 strong). The histologic results are added to Table 1.

RGD PET was performed in all of enrolled patients and all of tumor lesions showed discernible RGD uptake. SUV_{tumor} was 2.7±0.7 (range 1.4-4.8) and SUV_{normal} was 1.5±0.5 (range 0.7-2.9). Calculated TBR was 2.0±0.6

(range 0.9-3.2).

Functional MRI data was available in 33 patients. Quantitative parameters including K_{trans}, V_e, K_{ep} and $_{i}$AUC were successfully obtained from DCE MRI. Overall K_{trans} was 0.27±0.15 (range 0.02-0.55), V_e was 0.43±0.23 (range 0.02-0.82), K_{ep} was 0.79±0.60 (range 0.18-2.58) and $_{i}$AUC was 30.58±19.74 (range 3.15-73.29). ADC_{Mean} calculated from ADC map was 1.046±0.302 (range 0.279-1.566).

TABLE 1. Clinical and histopathologic characteristics of patients.

Clinical Features	Pts' No.	Histologic Results	Pts' No.
Tumor size		HER2	
2 cm and less	1	Negative	24
2–5 cm	20	Positive	13
> 5 cm	16	HER1/EGFR	
LN involvement		Negative	23
Negative	6	Positive	8
Positive	31	VEGF	
Clinical stage		Negative	0
IIb	13	Weak	7
IIIa	9	Strong	13
IIIb	12		
IIIc	3		
ER			
Negative	17		
Positive	18		
PR			
Negative	21		
Positive	14		

ER=estrogen receptor; PR=progesterone receptor; HER=human epidermal growth factor receptor; VEGF=vascular endothelial growth factor

2. Clinical and Quantitative Imaging Parameters According to HER Status

Between HER2 positive and negative group, TBR resulted significant difference. HER2 positive group showed 2.4±0.5 (range 1.7-3.2), while HER2 negative group showed 1.7±0.6 (range 0.9-2.9). TBR of HER2 positive group was significantly higher compared with HER2 negative group (p=0.002) (Fig. 1).

Any of clinical parameters did not show statistically significant difference between HER2 positive and negative group. However, regarding tumor size, increase tendency was detected in HER2 positive group compared with negative group (5.4±2.7 vs. 4.8±1.6, p=0.69). Regarding lymph node status, proportion of lymph node positive patient was larger in HER2 positive group compared with negative group (92.3% vs. 79.2%, p=0.394). In the aspect of clinical stage, proportion of stage III was larger in positive group than negative group (76.9% vs. 58.3%, p =0.228). Proportion of ER negative patient was slightly larger in positive group than negative group (58.3% vs. 43.4%, p=0.489). These results are summarized in Table 2.

Regarding HER1/EGFR expression, clinical stage and TBR quantitative RGD PET parameter resulted significant difference between 2 groups. TBR in

HER1/EGFR positive group was significantly higher than negative group (3.4±1.7 vs. 1.7±0.6, p<0.001) (Fig. 1). And proportion of clinical stage III in HER1/EGFR positive group was significantly larger than negative group (p=0.023) (Table 2).

Any of DCE MRI-derived quantitative parameters did not showed statistical significances between 2 groups. However, K_{trans} showed slightly increase tendency (0.283±0.130 vs. 0.269±0.146, p=0.674 for HER2; 0.282 ±0.131 vs. 0.262±0.142, p=0.872 for HER1/EGFR), V_e showed increase tendency (0.477±0.231 vs. 0.403±0.228, p=0.321 for HER2), and $_{i}$AUC showed increase tendency (38.3±19.9 vs. 26.7±18.9, p=0.166 for HER2; 37.4±19.2 vs. 30.1±19.2, p=0.720 for HER1/EGFR) in HER positive group compared with negative group (Fig. 2).

From DW imaging, ADC_{Mean} value showed slightly decrease tendency in HER positive group compared to negative group (1.029±0.328 vs. 1.055±0.296, p=0.647 for HER2; 0.892±0.330 vs. 1.134±0.250, p=0.182 for HER1/EGFR), though no statistical significance was observed (Fig. 3).

Comparison between HER positive and negative group according to each quantitative parameter was also summarized in Table 2. And the images of example cases were demonstrated in Figure 4.

Figure 1.

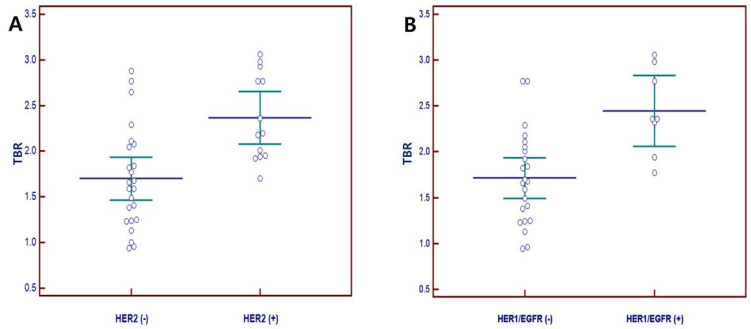

FIGURE 1 Comparison between HER positive and negative group according to quantitative imaging parameter, TBR, derived from ^{68}Ga-RGD PET/CT (A: HER2; B: HER1/EGFR). Horizontal line indicates mean and error bar indicates 95% confidence interval (CI) for mean.

Figure 2.

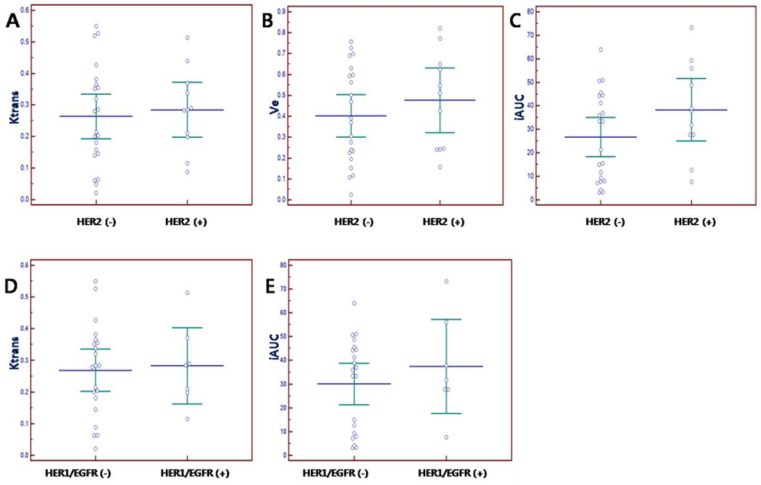

FIGURE 2 Comparison between HER positive and negative group according to quantitative imaging parameters derived from Dynamic Contrast Enhanced MRI (A, B, C: HER2; D, E: HER1/EGFR). Horizontal line indicates mean and error bar indicates 95% confidence interval (CI) for mean.

Figure 3.

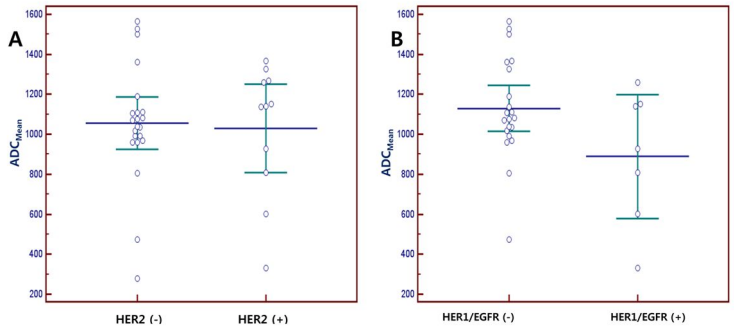

FIGURE 3 Comparison between HER positive and negative group according to quantitative imaging parameters derived from Diffusion Weighted MRI (A: HER2; B: HER1/EGFR). Horizontal line indicates mean and error bar indicates 95% confidence interval (CI) for mean.

Figure 4.

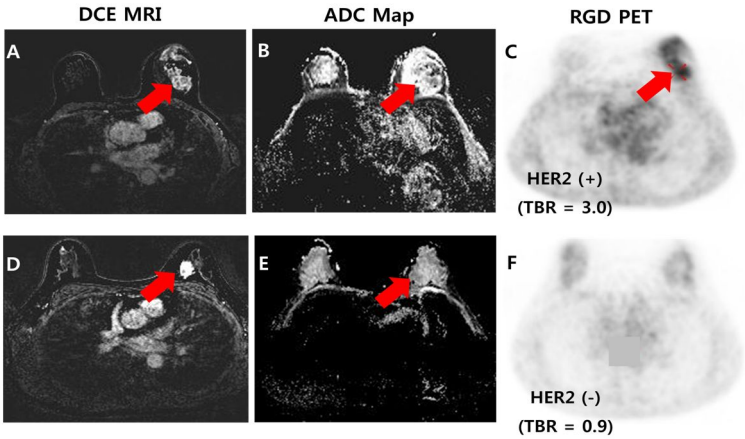

FIGURE 4 The representative images of HER2 positive patient (A: DCE MRI; B: DW MRI; C: RGD PET) and HER2 negative patient (D: DCE MRI; E: DW MRI; F: RGD PET). HER2 (+) patient shows higher TBR compared with HER2 (−) patient (C and F). K_{trans}, V_e and $_{i}$AUC parameter of HER2 (+) patient was slightly higher than HER2 (−) patient (0.370 vs. 0.355, 0.512 vs. 0.225 and 56.001 vs. 35.934)(A and D). ADC_{Mean} of HER2 (+) patient was slightly lower than HER2 (−) patient (0.601 vs. 0.993) (B and E).

TABLE 2. Clinical and quantitative imaging parameters regarding ErbB receptor status

	HER2			HER1/EGFR		
	Negative	Positive	*p*	Negative	Positive	*P*
Clinical factors (n=37 for HER2, n=31 for HER1/EGFR)						
†Tumor	4.8±1.6	5.4±2.7	0.69	4.9±2.2	5.4±2.2	0.49
LN status			0.39			0.61
(−)	5	1		4	1	
(+)	19	12		19	7	
cStage			0.23			0.02*
II	10	3		10	1	
III	14	10		13	7	
ER status			0.49			0.18
(−)	10	7		11	6	
(+)	13	5		12	2	
RGD PET parameters (n=37 for HER2, n=31 for HER1/EGFR)						
TBR	1.7±0.7	3.0±1.4	0.002*	1.7±0.6	3.4±1.7	<0.001*
DCE MRI parameters (n=33 for HER2, n=29 for HER1/EGFR)						
‡K_{trans}	0.26±0.15	0.28±0.13	0.67	0.26±0.14	0.28±0.13	0.87

V_e	0.40±0.23	0.48±0.23	0.32	0.41±0.24	0.40±0.17	0.84
‡K_{ep}	0.84±0.70	0.68±0.31	0.84	0.82±0.63	0.79±0.35	0.34
$_{i}$AUC	26.7±18.9	38.3±19.9	0.17	30.1±19.2	37.4±19.2	0.72
DW MRI parameters (n=33 for HER2, n=29 for HER1/EGFR)						
‡ADC_{Mean}	1.06±0.30	1.03±0.33	0.65	1.13±0.25	0.89±0.33	0.18

†cm for size; ‡min^{-1} for K_{trans}, K_{ep} and 10^{-3} mm^2/s for ADC_{Mean}

Chi-square or Fisher's exact test for un-continuous parameters; Mann-Whitney test for continuous parameters; $*p<0.05$

3. Predictive Performance Evaluation using ROC Curve

Predictive performance of TBR for HER2 over-expression was assessed with ROC analysis. The plotted curve is demonstrated in Figure 5. With the cut-off value of 1.84, sensitivity of 92.3%, specificity of 70.8%, positive predictive value (PPV) of 63.2%, and negative predictive value (NPV) of 94.4% was resulted (AUC of 0.849). Regarding HER1/EGFR expression, TBR resulted in 87.5% sensitivity, 69.6% specificity, 50.0% PPV, and 94.1% NPV with 1.92 cut-off value (AUC of 0.870).

Figure 5.

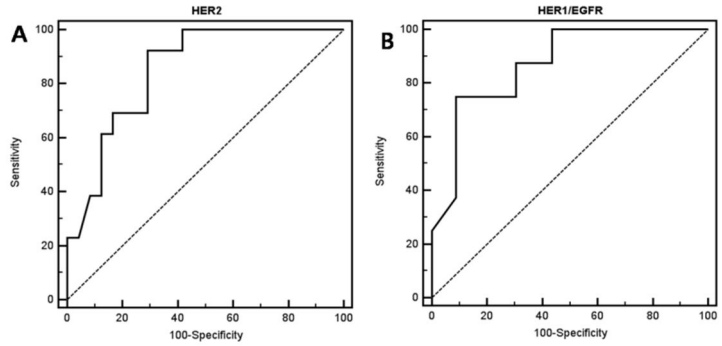

FIGURE 5 ROC curves of TBR for HER2 (A) and HER1/EGFR (B) status prediction.

4. Correlation of Imaging Parameter with HER2/CEP17 Ratio

Because 28 patients were referred to FISH analysis to confirm HER2 over-expression, HER2/CEP17 ratio can be used as a continuous variable in this group.

From simple correlation analysis, moderate positive correlation between TBR and HER2/CEP17 ratio was observed (r=0.641, p<0.001), while moderate negative correlation between ADC_{Mean} and HER2 ratio was observed (r=-0.653, p<0.001). Otherwise, no correlation was found with clinical and DCE MRI-derived parameters. The scatter plots are demonstrated on Figure 6.

As we can see from Figure 6 scatter plots, two discriminative subgroups were existed; HER2 positive and negative group. Because these two subgroups showed grossly distinguishable distribution pattern, we performed regression analysis regarding subgroup as well as total group and compared predictive strength of each regression equation.

The predictive strength (R^2) of TBR and ADC_{Mean} against HER2/CEP17 ratio was 0.41 and 0.43, respectively, for total group. When the regression equation was generated for limited HER2 positive subgroup, R^2 value was improved from 0.41 to 0.71 for TBR (Fig. 7A) and from 0.43 to

0.79 for ADC_{Mean} (Fig. 7B). However, almost no predictive strength of TBR (R^2=0.16) and ADC_{Mean} (R^2=0.05) parameter was observed when the regression equation was generated for limited HER2 negative subgroup (Fig. 7C and 7D). Furthermore, we hypothesized optimal model for HER2/CEP17 ratio prediction with quantitative imaging parameters including both TBR and ADC_{Mean} regarding limited HER2 positive group. With multiple regression analysis, R^2 value was improved to 0.84 (p=0.011). All of regression results are summarized in Table 3.

Figure 6.

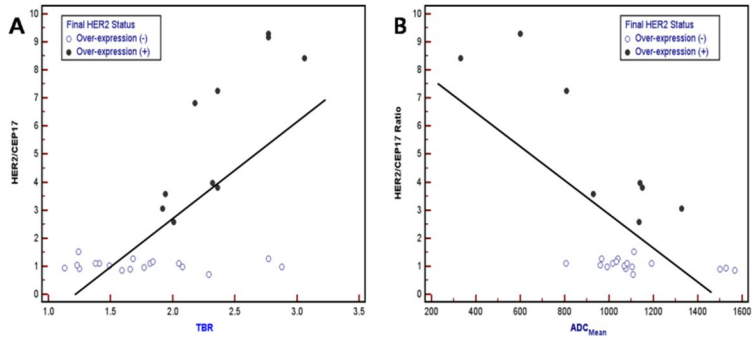

FIGURE 6 Scatter plots between quantitative imaging parameters (A: TBR; B: ADC_{Mean}) and HER2/CEP17 ratio in total group. Filled-in circle indicates HER2 over-expression positive case, while blank circle indicates HER2 over-expression negative case. Regression line is also shown.

Figure 7.

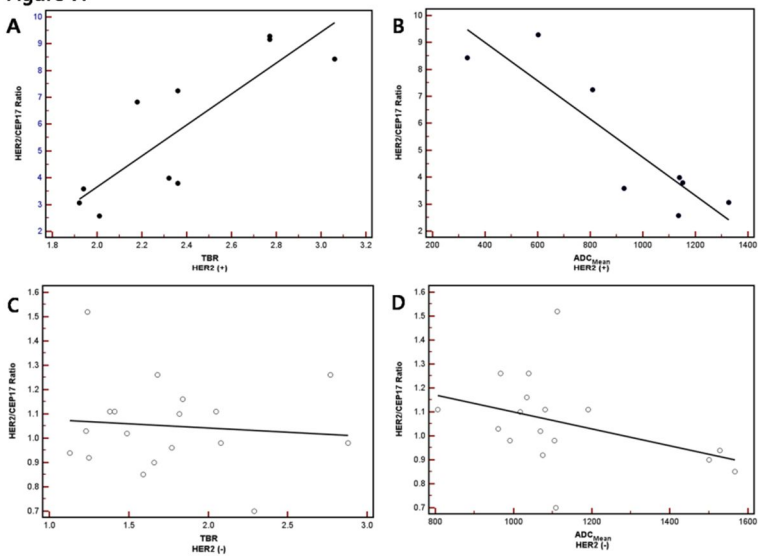

FIGURE 7 Scatter plot with regression line between quantitative imaging parameters (A, C: TBR; B, D: ADC_{Mean}) and HER2/CEP7 ratio in subgroup: HER2 over-expression (+) subgroup (A and B) and HER2 over-expression (-) subgroup (C and D).

TABLE 3. Outcome of regression analysis for total and subgroup

Simple Regression Outcome									
	Total group			HER2 (+) subgroup			HER2 (−) subgroup		
	Slope	*P*	R^2	Slope	*P*	R^2	Slope	*P*	R^2
TBR	3.25	<0.001	0.411	5.78	0.002	0.708	−0.04	0.711	0.009
ADC_{Mean}	−0.01	<0.001	0.427	−0.01	0.003	0.794	0.00	0.159	0.112

Multiple regression outcome									
	Total group			HER2 (+) subgroup			HER2 (−) subgroup		
	Slope	*P*	R^2	Slope	*P*	R^2	Slope	*P*	R^2
TBR	1.62	0.04		2.65	0.29		−0.06	0.45	
			0.525			0.837			0.194
ADC_{Mean}	−0.01	0.01		−0.01	0.18		0.00	0.09	

Slope; Coefficient value, *p* value; Refers to the individual statistical significance of TBR and ADC_{Mean} within their respective regression equations, R^2; Coefficient of determination

5. Correlation of Imaging Parameter with Angiogenic Biomarker

VEGF expression was identified in 20 patients. Of 20 specimens, 13 were pre-surgical biopsy specimens and 7 were post-surgical specimens. The VEGF result from biopsy specimen was analyzed with imaging parameters derived from initial staging imaging, while VEGF result from post-surgical specimen was analyzed with imaging parameters derived from pre-surgical follow up imaging.

All of 20 patients showed positive VEGF expressions. According to visual grading method, 13 patients were categorized as strong VEGF expression, while 7 patients were belonged to weak VEGF expression. Strong VEGF group presented significantly higher TBR compared to weak VEGF group (2.47 ± 0.63 vs. 1.77 ± 0.49, $p=0.016$) (Fig. 8). However, no significant correlations were noted between VEGF expression and other quantitative imaging parameters from functional MRI (Fig. 9).

Figure 8.

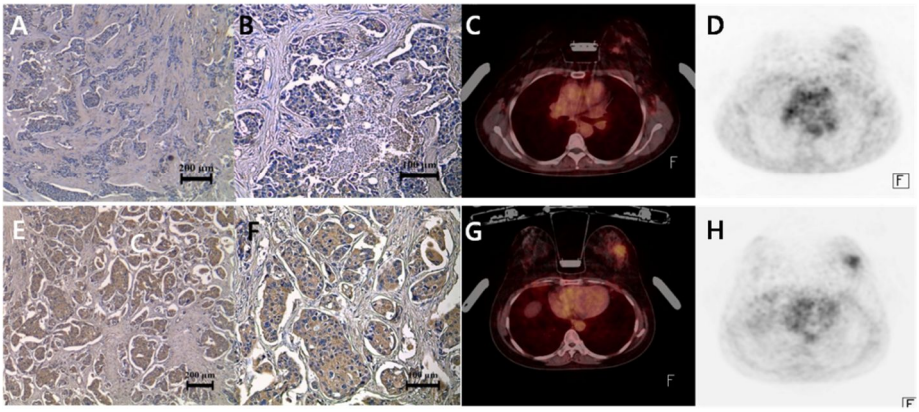

FIGURE 8 Example of "weak VEGF expression + low TBR" patient (A, B, C, and D) and "strong VEGF expression + high TBR" patient (E, F, G, and H). (A & E) VEGF (x 100), (B & F) VEGF (x 200), (C & G) ^{68}Ga-RGD PET/CT fusion image, (D & H) ^{68}Ga-RGD PET image. Positive staining of VEGF manifested itself as a cytoplasmic staining filled with brown color. In the case of "weak VEGF expression + low TBR", only small portion of cytoplasm of tumor cell was stained with brown (A & B) and TBR of 1.77 was measured from left breast tumor mass (C & D). Meanwhile, in the case of "strong VEGF expression + high TBR", most of cytoplasm of tumor cell was filled with dark brown (E & F) and TBR of 3.40 was measured from left breast tumor mass (G & H).

Figure 9.

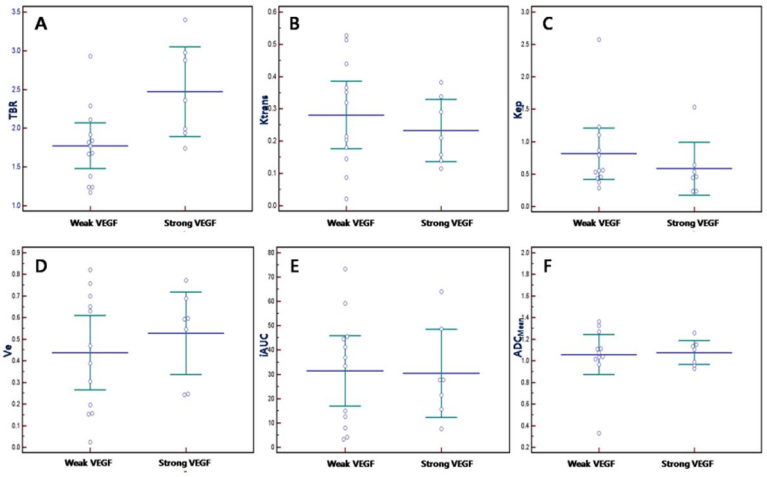

FIGURE 9 Comparison between strong VEGF group and weak VEGF group according to quantitative imaging parameters (A: TBR, B: K_{trans}, C: K_{ep}, D: V_e, E: $_{i}AUC$, F: ADC_{Mean}). Horizontal line indicates mean and error bar indicates 95% confidence interval (CI) for mean.

6. Correlations between HER Status and VEGF Expression

No direct correlation was noted between HER2 expression status and VEGF expression. Though the proportion of patients with strong VEGF expression was larger in HER2 positive group compared to negative group (50.0% vs. 25.0%, p=0.36), statistical significance was not noted. However, HER1/EGFR positive group showed significantly higher proportion of strong VEGF expression compared to negative group (75.0% vs. 16.7%, p=0.06). These results are summarized as frequency chart (Fig. 10).

Figure 10.

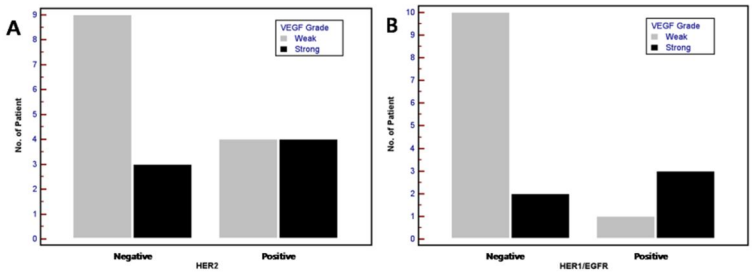

FIGURE 10 Frequency chart between HER status and VEGF expression (A: HER2, B: HER1/EGFR).

IV. DISCUSSION

This study purposed to predict pathologic biomarker expression, especially HER2 and HER1/EGFR, by using functional imaging modalities including ^{68}Ga-RGD PET/CT, DCE and DW MRI. Among used imaging parameters, TBR, which is derived from RGD PET/CT, showed significant higher value in HER2 positive group compared with HER2 negative group (p=0.002). Regarding HER1/EGFR, positive group resulted in significantly higher TBR compared with negative group (p<0.001). According to ROC analysis, TBR can predict HER2 expression with 92.3% sensitivity, 70.8% specificity, 78.4% accuracy (AUC of 0.849) and HER1/EGFR expression with 87.5% sensitivity, 69.6% specificity 74.1% accuracy (AUC of 0.870).

RGD PET is a promising imaging modality to evaluate angiogenesis by reflecting $\alpha_v\beta_3$ integrin expression. ^{18}F-Galacto-RGD PET was performed in 19 heterogenous solid tumor patients and RGD uptake (SUV and tumor/blood ratio) was correlated with $\alpha_v\beta_3$ integrin expression as determined by immunohistochemistry (22). Imaging parameters of tumor RGD uptake showed significant correlation with the intensity of immunohistochemical staining as well as microvessel density (MVD), which is

a representative marker of angiogenesis. In patients with head and neck cancer, same study group demonstrated good tumor/background ratios with same RGD tracer and $\alpha_v\beta_3$ integrin expression was identified from immunohistochemistry (23).

Integrin is an important key factor in angiogenesis. Integrin is a transmembrane adhesion receptor that directly bind extracellular matrix (ECM) proteins or other adhesion receptors and participates in cell motility and invasion. Unlike quiescent endothelium, neoangiogenesis of tumor express integrin subtype $\alpha_v\beta_3$ (24). It has been proposed that over-expressed integrin receptors allow angiogenic endothelial cells to bind ECM proteins and these adhesive interactions provide traction for invading endothelial cells consisting tumor feeding vessels (25). Furthermore, integrin interact directly or indirectly with other key angiogenic molecules such as vascular endothelial growth factor (VEGF), fibroblast growth factor (FGF) (26).

The role of HER2 in angiogenesis has been studied for years. Because HER2 over-expressed tumor is highly expected to show aggressive tumor growth and frequent metastasis, it can be easily assumed that more active tumor angiogenesis will be required in HER2 over-expressed tumors. Even if the clear molecular pathway between angiogenesis and HER2 receptor

is still unbreathed, there exist preclinical and clinical evidences that HER2 receptor has close relationship with tumor angiogenesis. Petit et al (27) demonstrated that neutralizing antibodies against HER1/EGFR and HER2 reduces the expression of VEGF in human breast cancer cell lines. Studies by Russell et al (28) and Bagheri-Yarmand et al (29) provided evidence that the upregulation of VEGF pathway can be induced by neuregulin, an ErbB ligand. And study by Saucier et al (30) demonstrated comparatively detailed mechanism of HER2 receptor-related tumor angiogenesis through the activation of Shc adaptor protein-dependent pathway to promote enhanced VEGF expression. According to clinical reports from pathology department, significant correlation between HER2 expression and MVD was observed from tumor specimens of breast cancer patients (5). Vogl et al (31) also studied about correlations between HER family (HER/EGFR and HER2) and tissue angiogenic biomarkers (VEGF and MVD) in breast cancer patients. However, they reported that HER2 is unlikely to be involved in direct regulation of angiogenesis, while HER1/EGFR is the major modulating factor for angiogenesis.

According to our current results, high TBR was observed in HER2 positive group as well as HER1/EGFR positive group and these findings

coincide with high angiogenic potential in HER2 or HER1/EGFR over-expressed group. Moreover, our results imply of integrin's participation in the ErbB receptor-mediated angiogenic pathway. However, detailed mechanism should be clarified through in vitro and in vivo study in the future.

DCE MRI is an emerging method of investigating microvascular structure as well as function by tracking the dynamic pharmacokinetics of injected low molecular weight T1-shortening parametric contrast, gadolinium. This technique can detect alterations in vascular permeability, extravascular extracellular volume, intravascular volume and blood flow with high sensitivity (12, 32). Semi-quantitative initial area under curve ($_{i}$AUC) obtained from contrast agent concentration-time curve and quantitative parameters derived from complex analysis methods including pharmacokinetic modeling are currently used; (1) The transfer constant, K_{trans}, (2) The extravascular extracellular space volume, V_e, (3) The rate constant, K_{ep}, calculated from K_{trans}/V_e. K_{trans}, V_e, $K_{ep,}$ and $_{i}$AUC are generally higher in breast cancers due to high permeability of immature tumor vascular structure. And significant reductions in these parameters indicate favorable treatment response in breast cancer (33-35).

Although both of RGD PET and DCE MRI are functional imaging

modalities reflecting tumor angiogenesis, this study could not find any statistically reliable correlations between ErbB receptor expression and DCE MRI-derived parameters. This discordance can be explained from multi-step mechanism of tumor neovascularization. Because integrin participated in angiogenesis by vascular endothelial cell migration and invasion, RGD PET can theoretically reflect angiogenic activity from early stage of angiogenesis. However, alteration of vascular permeability which is assessed from DCE MRI is only a product of immature tumor vasculature and cannot provide information along with whole process of angiogenesis. Small number of enrolled patients should be considered as another cause. K_{trans}, V_e and $_iAUC$ showed slightly increase tendency in HER2 positive group compared with negative group, even if without statistical significance. In the case of HER1/EGFR, K_{trans} and $_iAUC$ showed increase tendency in positive group compared to negative group.

Because fluorescence in situ hybridization (FISH) is known to be more accurate than IHC for HER2 status determination in breast cancer, the preferred analysis protocol is IHC with FISH as a follow up test for equivocal results (36, 37). Our study also followed the recommended protocol and additional FISH analysis was performed in the case of ambiguous IHC result.

Total of 28 patients were available with HER2 gene amplification ratio data. Additional analysis about the correlation between gene ratio and each imaging biomarker was performed. Simple correlation analysis resulted in moderate positive correlation between TBR and gene ratio (r=0.641, p<0.001), whereas moderate negative correlation between ADC_{Mean} and gene ratio (r=−0.653, p<0.001).

The role of DW MRI, which is based on water diffusion, is gradually increasing in oncologic fields and being explored to aid not only diagnosis but also treatment response evaluation (38−40). DW MRI is known to provide information about tumor cell density, cell membrane integrity. ADC value derived from DW MRI reflects the free diffusion of water molecules in extracellular space; this generally results in reduced ADC value in tumors with high cell density and negative correlation with histologic grade (41−43). Because HER2 gene amplification is an established poor prognostic factor owing to its highly aggressiveness in breast carcinoma, negative correlation between ADC_{Mean} and HER2 gene ratio have a thread of connection with previous studies.

Despite of moderate degree correlations, both of scatter plots (TBR vs. HER2 gene ratio and ADC_{Mean} vs. HER2 gene ratio) showed distinguishable

distributional patterns between finally confirmed HER2 positive and negative group. On the basis of scatter plot finding, regression analysis regarding each subgroup as well as total group was performed and predictive strength (R^2 value) of each other was assessed. The predictive strength of TBR and ADC_{Mean} in limited HER2 positive subgroup improved about two-fold compared with total group (R^2 =0.41 to 0.71 for TBR and R^2 =0.43 to 0.79 for ADC_{Mean}), while almost no predictive strength was observed in limited HER2 negative subgroup (R^2= 0.01 for TBR and R^2=0.11 for ADC_{Mean}). In HER2 negative subgroup, patients with low HER2 gene amplification showed wide range of TBR and ADC_{Mean} (Fig. 7C and 7D). Because numerous key factors participated in angiogenesis and tumor progression, other regulatory process bypassing HER2 over-expression could exist in those patients. Anyway, these results indicate that the potential utility of TBR and ADC_{Mean} as an imaging biomarker for noninvasive prediction of HER2 gene amplification, especially in the case of finally confirmed HER2 positive cases that would be candidates for trastuzumab treatment. Application of imaging biomarker for HER2 expression can potentialize non-invasive and early prediction of tumor response during trastuzumab treatment, even if initial biopsy is still needed for not only HER2 status but also other prognostic tissue biomarker

confirmation before therapy.

To confirm the relationship between RGD uptake and angiogenic activity, this study further investigated the histologic expression of VEGF, the representative angiogenic marker, from tissue specimens of enrolled patients.

Because VEGF was not included in initial work up for histologic biomarker identification, the re-cut section of residual paraffin block was requested at our pathology department. The pre-surgical biopsy can obtain only small amount of tissue specimen. Therefore, in the case of insufficient amount of residual paraffin block for additional re-cut section, post-surgical specimens were used. This point can be a limitation of this study. To catch up this limitation, pre-surgical imaging, which was performed at the end of neoadjuvant chemotherapy, was used to analyze the correlation of VEGF expression from post-surgical specimen with imaging parameters. Finally, 20 specimens consisted of 13 pre-treatment and 7 post-surgical ones were available for additional VEGF expression identification.

As a result, TBR showed significant positive correlation with VEGF expression (p=0.016). From the representative images (Fig. 8), stong VEGF expression (cytoplasmic filling with brown color) was identified from high TBR case, while weak VEGF expression was identified from low TBR case.

Thus, RGD PET can predict angiogenic activity by reflecting VEGF expression. If this preliminary result is validated in larger group of patients, RGD PET can be used as the promising tool for treatment response evaluation during anti-angiogenic therapy such as bevacizumab.

This study further investigated about the association of VEGF expression with HER expression status. The proportion of strong VEGF expression was larger in HER2 positive group, but statistical significance was not noted. Meanwhile, significant positive correlation was noted between HER1/EGFR and VEGF expression (p=0.06). Although it has been suggested that the upregulation of VEGF can be modulated by HER2 expression (44-46), this study could not show a coincident result. It is probably due to numerous key factors will exist in the molecular pathway between HER2 and VEGF expression, because angiogenesis is extremely complex mechanism. According to study by Vogl et al., they found significant correlation between HER1/EGFR and MVD as well as high VEGF expression, while the relationship with HER2 was not significant (31). The receptor dimerization of HER2 and HER1/EGFR is though to regulate molecular signaling pathways responsible for multiple biologic function including neovascularization of tumor in breast cancer (3, 47). These results may indicate that cooperation between HER2

and HER1/EGFR regulate angiogenic pathway, so even HER2 over-expression negative patients did show strong VEGF expression.

V. REFERENCES

1. Ross JS, Fletcher JA, Linette GP, Stec J, Clark E, Ayers M, et al. The Her-2/neu gene and protein in breast cancer 2003: biomarker and target of therapy. The oncologist. 2003;8(4):307-25.

2. Bargmann CI, Hung MC, Weinberg RA. The neu oncogene encodes an epidermal growth factor receptor-related protein. Nature. 1986;319(6050):226-30.

3. Yen L, Benlimame N, Nie ZR, Xiao D, Wang T, Al Moustafa AE, et al. Differential regulation of tumor angiogenesis by distinct ErbB homo-and heterodimers. Molecular biology of the cell. 2002;13(11):4029-44.

4. Kumar R, Yarmand-Bagheri R, editors. The role of HER2 in angiogenesis2001: Elsevier.

5. Vamesu S. Angiogenesis and c-erbB-2 (HER2/neu) overexpression status in primary breast cancer patients: an analysis of 158 needle core biopsies. Rom J Morphol Embryol. 2007;48(2):121-9.

6. Batchelor TT, Sorensen AG, Di Tomaso E, Zhang WT, Duda DG, Cohen KS, et al. AZD2171, a pan-VEGF receptor tyrosine kinase inhibitor, normalizes tumor vasculature and alleviates edema in glioblastoma patients.

Cancer cell. 2007;11(1):83-95.

7. Chen W, Delaloye S, Silverman DHS, Geist C, Czernin J, Sayre J, et al. Predicting treatment response of malignant gliomas to bevacizumab and irinotecan by imaging proliferation with [18F] fluorothymidine positron emission tomography: a pilot study. Journal of Clinical Oncology. 2007;25(30):4714-21.

8. Willett CG, Duda DG, di Tomaso E, Boucher Y, Ancukiewicz M, Sahani DV, et al. Efficacy, safety, and biomarkers of neoadjuvant bevacizumab, radiation therapy, and fluorouracil in rectal cancer: a multidisciplinary phase II study. Journal of Clinical Oncology. 2009;27(18):3020-6.

9. Zhu AX, Sahani DV, Duda DG, Di Tomaso E, Ancukiewicz M, Catalano OA, et al. Efficacy, safety, and potential biomarkers of sunitinib monotherapy in advanced hepatocellular carcinoma: a phase II study. Journal of Clinical Oncology. 2009;27(18):3027.

10. Beer AJ, Kessler H, Wester HJ, Schwaiger M. PET imaging of integrin αvβ3 expression. Theranostics. 2011;1:48.

11. Turkbey B, Thomasson D, Pang Y, Bernardo M, Choyke PL. The role of dynamic contrast-enhanced MRI in cancer diagnosis and treatment. Diagn Interv Radiol. 2010;16:186-92.

12. O'Connor JPB, Jackson A, Parker GJM, Jayson GC. DCE-MRI biomarkers in the clinical evaluation of antiangiogenic and vascular disrupting agents. British journal of cancer. 2007;96(2):189-95.

13. Weis SM, Cheresh DA. αv Integrins in Angiogenesis and Cancer. Cold Spring Harbor Perspectives in Medicine. 2011;1(1).

14. Arthurs OJ, Gallagher FA. Functional and molecular imaging with MRI: potential applications in paediatric radiology. Pediatric radiology. 2011;41(2):185-98.

15. Neeman M, Dafni H. Structural, functional, and molecular MR imaging of the microvasculature. Annual review of biomedical engineering. 2003;5(1):29-56.

16. Hoff BA, Bhojani MS, Rudge J, Chenevert TL, Meyer CR, Galbán S, et al. DCE and DW-MRI monitoring of vascular disruption following VEGF-Trap treatment of a rat glioma model. NMR in Biomedicine. 2011.

17. Jung DC, Lee HJ, Seo JW, Park SY, Lee SJ, Lee JH, et al. Diffusion-Weighted Imaging of a Prostate Cancer Xenograft Model Seen on a 7 Tesla Animal MR Scanner: Comparison of ADC Values and Pathologic Findings. Korean Journal of Radiology. 2012;13(1):82.

18. Kim JH, Lee JS, Kang KW, Lee HY, Han SW, Kim TY, et al. Whole-

Body Distribution and Radiation Dosimetry of 68Ga-NOTA-RGD, a Positron Emission Tomography Agent for Angiogenesis Imaging. Cancer Biotherapy and Radiopharmaceuticals. 2011.

19. Wülfing P, Borchard J, Buerger H, Heidl S, Zänker KS, Kiesel L, et al. HER2-positive circulating tumor cells indicate poor clinical outcome in stage I to III breast cancer patients. Clinical cancer research. 2006;12(6):1715-20.

20. Lee SH, Cho N, Kim SJ, Cha JH, Cho KS, Ko ES, et al. Correlation between high resolution dynamic MR features and prognostic factors in breast cancer. Korean Journal of Radiology. 2008;9(1):10.

21. Wolff AC, Hammond MEH, Schwartz JN, Hagerty KL, Allred DC, Cote RJ, et al. American Society of Clinical Oncology/College of American Pathologists guideline recommendations for human epidermal growth factor receptor 2 testing in breast cancer. Archives of pathology & laboratory medicine. 2007;131(1):18-43.

22. Beer AJ, Haubner R, Sarbia M, Goebel M, Luderschmidt S, Grosu AL, et al. Positron emission tomography using [18F] Galacto-RGD identifies the level of integrin 慣v棺3 expression in man. Clinical cancer research. 2006;12(13):3942-9.

23. Beer AJ, Grosu AL, Carlsen J, Kolk A, Sarbia M, Stangier I, et al. [18F]

Galacto-RGD positron emission tomography for imaging of 慣v棺3 expression on the neovasculature in patients with squamous cell carcinoma of the head and neck. Clinical cancer research. 2007;13(22):6610-6.

24. Brooks PC, Clark R, Cheresh DA. Requirement of vascular integrin alpha v beta 3 for angiogenesis. Science. 1994;264(5158):569.

25. Desgrosellier JS, Cheresh DA. Integrins in cancer: biological implications and therapeutic opportunities. Nature Reviews Cancer.10(1):9-22.

26. Friedlander M, Brooks PC, Shaffer RW, Kincaid CM, Varner JA, Cheresh DA. Definition of two angiogenic pathways by distinct 慣v integrins. Science. 1995;270(5241):1500-2.

27. Petit A, Rak J, Hung MC, Rockwell P, Goldstein N, Fendly B, et al. Neutralizing antibodies against epidermal growth factor and ErbB-2/neu receptor tyrosine kinases down-regulate vascular endothelial growth factor production by tumor cells in vitro and in vivo: angiogenic implications for signal transduction therapy of solid tumors. The American journal of pathology. 1997;151(6):1523.

28. Russell KS, Stern DF, Polverini PJ, Bender JR. Neuregulin activation of ErbB receptors in vascular endothelium leads to angiogenesis. American Journal of Physiology-Heart and Circulatory Physiology. 1999;277(6):H2205-H11.

29. Bagheri-Yarmand R, Vadlamudi RK, Wang RA, Mendelsohn J, Kumar R. Vascular endothelial growth factor up-regulation via p21-activated kinase-1 signaling regulates heregulin-棺1-mediated angiogenesis. Journal of Biological Chemistry. 2000;275(50):39451-7.

30. Saucier C, Khoury H, Lai KMV, Peschard P, Dankort D, Naujokas MA, et al. The Shc adaptor protein is critical for VEGF induction by Met/HGF and ErbB2 receptors and for early onset of tumor angiogenesis. Proceedings of the National Academy of Sciences of the United States of America. 2004;101(8):2345.

31. Vogl G, Bartel H, Dietze O, Hauser-Kronberger C. HER2 is unlikely to be involved in directly regulating angiogenesis in human breast cancer. Applied Immunohistochemistry & Molecular Morphology. 2006;14(2):138.

32. AM O'Flynn E. Functional magnetic resonance: biomarkers of response in breast cancer. Breast Cancer Research. 2011;13(1):204.

33. Jayson GC, Zweit J, Jackson A, Mulatero C, Julyan P, Ranson M, et al. Molecular imaging and biological evaluation of HuMV833 anti-VEGF antibody: implications for trial design of antiangiogenic antibodies. Journal of the National Cancer Institute. 2002;94(19):1484-93.

34. Overmoyer B, Silverman P, Leeming R, Shenk R, Lyons J, Ziats N, et al.

Phase II trial of neoadjuvant docetaxel with or without bevacizumab in patients with locally advanced breast cancer. J Clin Oncol. 2004;22:727.

35. Wedam SB, Low JA, Yang SX, Chow CK, Choyke P, Danforth D, et al. Antiangiogenic and antitumor effects of bevacizumab in patients with inflammatory and locally advanced breast cancer. Journal of Clinical Oncology. 2006;24(5):769-77.

36. Ellis C, Dyson M, Stephenson T, Maltby E. HER2 amplification status in breast cancer: a comparison between immunohistochemical staining and fluorescence in situ hybridisation using manual and automated quantitative image analysis scoring techniques. Journal of clinical pathology. 2005;58(7):710-4.

37. Ellis I, Dowsett M, Bartlett J, Walker R, Cooke T, Gullick W, et al. Recommendations for HER2 testing in the UK. Journal of clinical pathology. 2000;53(12):890-2.

38. Pickles MD, Gibbs P, Lowry M, Turnbull LW. Diffusion changes precede size reduction in neoadjuvant treatment of breast cancer. Magnetic resonance imaging. 2006;24(7):843-7.

39. Sharma U, Danishad KKA, Seenu V, Jagannathan NR. Longitudinal study of the assessment by MRI and diffusion-weighted imaging of tumor

response in patients with locally advanced breast cancer undergoing neoadjuvant chemotherapy. NMR in Biomedicine. 2009;22(1):104-13.

40. Nilsen L, Fangberget A, Geier O, Olsen DR, Seierstad T. Diffusion-weighted magnetic resonance imaging for pretreatment prediction and monitoring of treatment response of patients with locally advanced breast cancer undergoing neoadjuvant chemotherapy. Acta Oncologica. 2010;49(3):354-60.

41. Woodhams R, Matsunaga K, Kan S, Hata H, Ozaki M, Iwabuchi K, et al. ADC mapping of benign and malignant breast tumors. Magnetic resonance in medical sciences: MRMS: an official journal of Japan Society of Magnetic Resonance in Medicine. 2005;4(1):35.

42. Partridge SC, DeMartini WB, Kurland BF, Eby PR, White SW, Lehman CD. Differential diagnosis of mammographically and clinically occult breast lesions on diffusion-weighted MRI. Journal of Magnetic Resonance Imaging. 2010;31(3):562-70.

43. Bogner W, Gruber S, Pinker K, Grabner G, Stadlbauer A, Weber M, et al. Diffusion-weighted MR for Differentiation of Breast Lesions at 3.0 T: How Does Selection of Diffusion Protocols Affect Diagnosis? 1. Radiology. 2009;253(2):341-51.

44. Eccles SA. The role of c-erbB-2/HER2/neu in breast cancer progression and metastasis. Journal of mammary gland biology and neoplasia. 2001;6(4):393-406.

45. Yang W, Klos K, Yang Y, Smith TL, Shi D, Yu D. ErbB2 overexpression correlates with increased expression of vascular endothelial growth factors A, C, and D in human breast carcinoma. Cancer. 2002;94(11):2855-61.

46. Konecny GE, Meng YG, Untch M, Wang HJ, Bauerfeind I, Epstein M, et al. Association between HER-2/neu and vascular endothelial growth factor expression predicts clinical outcome in primary breast cancer patients. Clinical cancer research. 2004;10(5):1706-16.

47. Earp HS, Dawson TL, Li X, Yu H. Heterodimerization and functional interaction between EGF receptor family members: a new signaling paradigm with implications for breast cancer research. Breast cancer research and treatment. 1995;35(1):115-32.

국문초록

목적: HER2 과다발현을 보이는 유방암은 빠른 종양 성장 및 잦은 임파선 전이를 보이는 것으로 알려져 있다. 이러한 환자들은 Trastuzumab 치료의 대상이 된다. 한편, HER1/EGFR는 DNA 서열의 많은 부분이 HER2와 일치하는 것으로 알려져 있다. 본 전향적 연구는 신생혈관생성을 반영하는 기능적 영상으로부터 얻어진 정량적 지표들과 면역병리를 통해 확인된 외피성장인자수용체 (Human epidermal growth factor receptor, HER) 발현 간의 상관관계를 알아보고자 하였다. 또한, 정량적 영상 지표들과 대표적 신생혈관마커인 혈관내피성장인자 (Vascular endothelial growth factor, VEGF)와의 연관성을 알아보고자 하였다.

연구방법: 37명의 국소진행유방암 환자들이 연구에 포함되었다 (47.8 ± 7.6 세). ^{68}Ga 표지 RGD PET/CT, 동적조영증강 및 확상강조 MRI을 치료 전에 시행하였다. RGD PET으로부터 얻어진 종양 대 배후 섭취비 (Tumor to Background Ratio, TBR), 동적조영증강 MRI로부터 얻어진 K_{trans}, V_e, K_{ep}, $_{i}$AUC, 확산강조 MRI로부터 얻어진 ADC_{Mean}을 정량적 영상 지표로 이용하였다. 또한 임상적 지표로서 원발종양의 크기, 임파절 전이 유무, 임상적 병기, 호르몬 수용체 발현 여부를 평가하였다. 모든 환자에서 중심부 바늘생검을 시행하였다. HER1/EGFR의 조직학적 발현을 확인하기 위해 면역화학적 염색을 시행하였다. HER2 발현의 정확한 평가를 위해 면역화학적 염색을 시행하였고, 그 결과가 불확실할 경우에

추가적 형광동소보합법 (Fluorescence in situ hybridization, FISH)을 시행하였다. 각각의 임상 및 정량적 영상 지표들과 HER 발현 간의 상관관계를 분석하였으며, 이들 지표들의 HER 발현에 대한 예측정도를 평가하기 위해 선형 회귀 분석 및 수용자 반응 특성 (reciever operating characteristics, ROC) 곡선 분석을 시행하였다. 나아가, 영상 지표들과 대표적 신생혈관마커인 VEGF 간의 연관성을 평가하기 위해 VEGF에 대한 면역화학적 염색 및 상관관계 분석을 추가적으로 시행하였다.

결과: HER2 과다발현이 37명 중 13명에서 확인되었고, HER1/EGFR은 31명 중 8명에서 확인되었다. HER 발현과 TBR이 유의한 상관관계를 보였다 (p<0.001, HER1/EGFR; p=0.002, HER2). 이에 반해 동적조영증강 및 확산강조 MRI로부터 얻어진 영상 지표들은 유의한 상관관계를 보이지 않았다. ROC 분석 결과, TBR은 92.3% 민감도, 70.8% 특이도로 HER2 발현을 예측하였으며 (AUC 0.849), 87.5% 민감도, 69.6% 특이도로 HER1/EGFR 발현을 예측하였다 (AUC 0.870). 총 28명의 환자에서 정확한 HER2 평가를 위해 추가적으로 FISH를 시행하였으며, HER2 유전자 증폭 정도를 나타내는 HER2/CEP17 ratio를 얻을 수 있었다 (2.7±2.8, range 0.7−9.3). TBR와 HER2/CEP ratio 간에 비교적 높은 정도의 양의 상관관계 (r=0.64, p=0.0002)가 관찰되었으며, ADC_{Mean}과 HER2/CEP ratio 간에 비교적 높은 정도의 음의 상관관계 (r=−0.65, p=0.0004)가 관찰되었다.

선형회귀분석 결과, 전체 그룹에서 HER2/CEP ratio에 대한 TBR와 ADC_{Mean}의

예측도는 각각 0.41과 0.43으로 높지 않았다. 그러나, HER2 양성 그룹만을 포함하였을 때 예측도는 각각 0.708과 0.794까지 향상되었다. 총 20명의 환자에서 보관된 병리 조직을 이용하여 VEGF 발현을 평가하였다. 오직 TBR만이 VEGF 발현정도와 유의한 상관관계를 보였다 (p=0.016). HER2와 VEGF 발현은 직접적 상관관계를 보이지 않았으나, HER1/EGFR은 유의한 상관관계를 보였다 (p=0.06).

결론: ^{68}Ga 표지 RGD PET과 확산강조 MRI을 이용하여 HER 바이오마커의 발현정도를 평가할 수 있겠다. 특히, 신생혈관생성을 반영하는 ^{68}Ga 표지 RGD PET은 HER2 및 HER1/EGFR 발현에 대하여 높은 예측도를 보였다. 따라서, 본 연구는 유방암에서 비침습적 주요 바이오마커 평가에 대한 기능적 영상의 잠재적 이용가치를 제시하였다. 뿐만 아니라, 본 연구를 통해 HER이 신생혈관생성의 경로에 관여하고 있음을 짐작할 수 있다.

주요어: RGD PET, 동적조영증강 MRI, 확산강조 MRI, 신생혈관생성, 유방암

학번: 2010-21810